TEMPERATURE DEPENDENCE OF MULTIMODE GALLIUM NITRIDE/ALUMINUM NITRIDE (GaN/AlN) HETEROSTRUCTURE STRING RESONATOR

Wen Sui[1], Xu-Qian Zheng[1], Ji-Tzuoh Lin[2], Bruce W. Alphenaar[2*], and Philip X.-L. Feng[1*]*
[1]Electrical and Computer Engineering, Herbert Wertheim College of Engineering, University of Florida, Gainesville, FL 32611, USA
[2]Electrical and Computer Engineering, University of Louisville, Louisville, KY 40292, USA

ABSTRACT

We report on the first experimental characterization and analysis of the temperature coefficient of resonance frequency (TC*f*) of gallium nitride/aluminum nitride (GaN/AlN) heterostructure doubly-clamped micro-string resonators with length L = 100 μm, thickness t = 700 nm, and width w = 5 μm. We observe three distinct resonances within the frequency range of 1.5 to 5 MHz at room temperature. Assisted by finite element method (FEM) simulations, we determine that the first two modes are out-of-plane flexural modes and the third one is an in-plane flexural mode, with the former two dominated by built-in stress and the latter one determined by both stress and flexural rigidity. We examine these resonances with varying temperature (-10 ºC to 105 ºC) and obtain TC*f*s of -336 ppm/K, -316 ppm/K, and -83 ppm/K for the three modes, respectively. The investigation provides essential information for thorough understanding of elastic behavior of GaN/AlN heterostructures upon temperature change.

KEYWORDS

GaN/AlN heterostructure, microelectromechanical systems (MEMS), resonator, temperature coefficient of resonance frequency (TC*f*), multimode resonator

INTRODUCTION

Gallium nitride (GaN) has been widely adopted in solid-state lighting and high-frequency and high-power electronics, especially for high temperature applications, thanks to its wide bandgap (E_g = 3.4 eV), p-type doping capability, high carrier mobility, and good thermal conductivity [1-3]. Endowed with high elastic modulus and piezoelectricity (Table 1), GaN has also stimulated growing interests in microelectromechanical systems (MEMS) and related applications [4]. Research focused upon integrating GaN MEMS transducers with GaN electronics is emerging to unlock the potential of GaN as an electromechanical material, which could lead to a step further in realizing advanced GaN integrated systems. GaN thin-film bulk acoustic resonator (FBAR) and MEMS resonator with integrated high electron mobility transistor (HEMT) channel have been demonstrated, suggesting new opportunities for high frequency applications [5,6]. In addition, monolithic integration of GaN MEMS with circuits could provide the advantages of small footprint and reduction of parasitics [4]. However, the columnar structure of GaN along with the lattice mismatch between GaN and the mainstream silicon (Si) substrate may induce localized strain near the interface, affecting the performance of GaN MEMS and electronic devices [7]. Although an AlN or AlN/AlGaN buffer layer can accommodate or mitigate the lattice mismatch and avoid chemical reactions between Ga and Si, stress gradient across the layers can often be generated upon cooling from growth temperature to room temperature, leading to warping or cracks. This may also influence the resonator performance for applications at changing or elevated temperatures. Further, the current flow in device could cause temperature increase due to Joule heating. The rising temperature will alter stress and Young's modulus, due to thermal expansion and constitutive crystals' temperature dependence of Young's modulus, respectively, and tune the resonance frequency of the structure. Such effect can be assessed by the temperature coefficient of frequency (TC*f*) [8]. The investigation of TC*f* could provide insight in analyzing how the fluctuations of temperature affects the performance of GaN MEMS, and GaN/AlN structures.

Table 1: Key material properties of AlN and GaN

Material	Young's Modulus [GPa]	Band Gap [eV]	Piezo-electric Constant [pm/V]	Thermal Conductivity [W/(m·K)]	Acoustic Velocity [m/s]
AlN	283–350	6.2	5.49	285	9320–10360
GaN	250–400	3.4	2.13	130	6780–8070

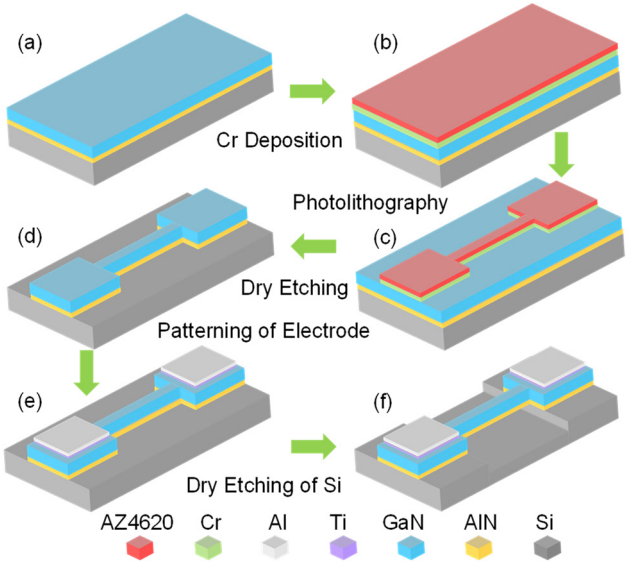

Figure 1: Microfabrication of the doubly-clamped GaN/AlN structures via a two-step lithographic process followed by device release in XeF_2 dry etching.

In this work, we present the first measurement of the TC*f* for both out-of-plane and in-plane flexural resonance modes in GaN/AlN doubly-clamped resonators by monitoring the temperature dependence of frequency in the range of -10 to 105 ºC. We fabricate the resonators by a two-step lithography process and measure the resonance response upon temperature change of the device using an ultrasensitive laser interferometry system.

DEVICE FABRICATION

We use GaN/AlN wafers (purchased from Kyma Technologies, Inc.) that consist of a crystalline GaN layer (500 nm) grown by hydride vapor phase epitaxy (HVPE) on top of an intermediate nucleation layer of AlN (200nm) on standard Si (111) substrate. As shown in Fig. 1, the fabrication of GaN/AlN strings starts from the deposition of chromium (Cr), followed by photo-lithography to define the Cr hard mask. We perform dry anisotropic etching with the Cr mask, through GaN and AlN layers, to define the doubly-clamped structures, followed by wet etching of Cr. After removal of Cr, we deposit and pattern the titanium (Ti) and aluminum (Al) electrode pads. Finally, we release the GaN/AlN heterostructure devices by isotropic dry etching of Si in xenon difluoride (XeF_2).

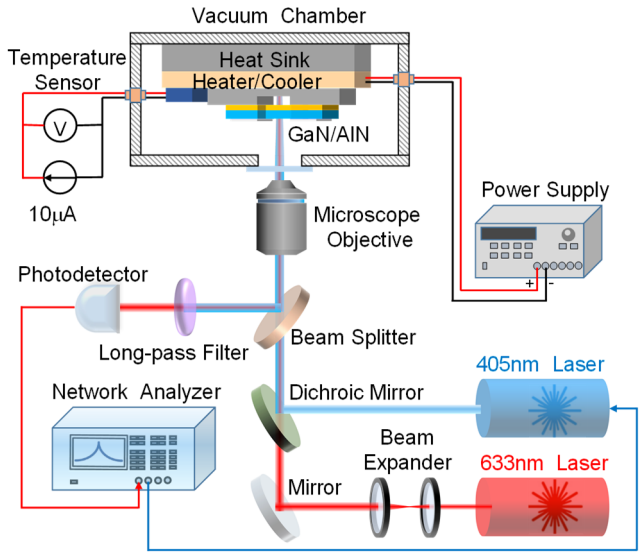

Figure 2: Illustration of the laser interferometry system with precisely temperature-controlled device stage.

MEASUREMENT TECHNIQUES

The multimode resonances of the GaN/AlN device are measured by using a laser interferometry system, as shown in Fig. 2. An intensity-modulated 405 nm blue diode laser is utilized to photothermally drive the device motion, and a 633 nm He-Ne laser is employed to detect the vibration. Dynamic interference happens between the light reflected by the vibrating string and that by the substrate surface below the suspended structure. Thus, the motion of the device is transduced by the interferometric effect into intensity variation of the reflected 633 nm light. The photodetector converts the optical signal into electrical signal, which is monitored by a network analyzer. We regulate the temperature of the GaN/AlN device by using a Peltier thermoelectric heater/cooler; and the temperature of the chip is measured by a Si diode temperature sensor (Lake Shore DT-670). We measure the resonance response of the device at different temperatures and extract the resonance frequency and quality (Q) factor of each mode by fitting the measured spectrum to the damped simple harmonic resonator model. All measurements are done in a moderate vacuum of ~80 mTorr.

RESULTS AND DISCUSSIONS

Figure 3 shows the measured multimode resonances in the range of 1.5 to 5 MHz, for a device with length $L \approx 100$ μm, thickness t = 700 nm and width $w \approx 5$ μm. Three resonance modes are observed, f_1 = 1.802 MHz, f_2 = 3.712 MHz, f_3 = 4.487 MHz. By matching the resonance frequencies to finite element method (FEM) simulation results, the first two modes are out-of-plane flexural modes while the third one is an in-plane flexural mode. To determine the TCf, we measure these modes in the temperature range of -10 to 105 ºC. The resonance frequencies of the three modes are recorded, and their TCf values are evaluated by using

$$\mathrm{TC}f = \frac{1}{f}\frac{df}{dT}, \qquad (1)$$

where T is temperature. The temperature coefficient of Young's modulus (TCE_Y) of a material is a contributing factor of TCf, which is determined by $\mathrm{TC}E_Y = (1/E_Y)(dE_Y/dT)$. In addition, variations in the device dimensions due to the linear thermal expansion coefficient (α) can alter the built-in stress and the geometry of the structure, and shift the resonance frequency. For example, using length of the structure, $\alpha = (1/L)(dL/dT)$.

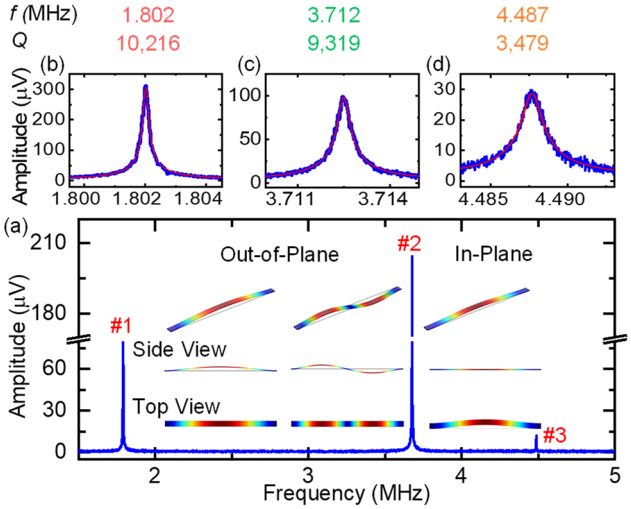

Figure 3: (a) Measured resonance spectra of a 100μm-long GaN/AlN string at room temperature with (b)-(d) showing the zoomed-in spectra of 3 modes with fitting. Insets show the corresponding simulated mode shapes.

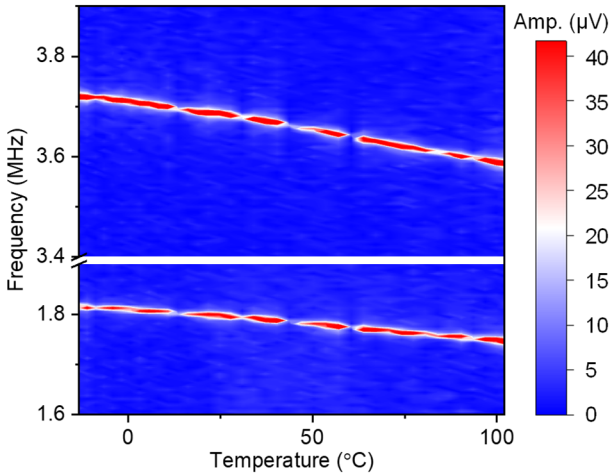

Figure 4: Color plot of the resonance spectra for the first two modes measured with varying temperature.

Figure 4 shows the resonance spectra of the first two

modes measured in temperature range of -10 to 105 ºC. We find that the resonance frequencies increase gradually with decreasing temperatures. By plotting the frequency shift at different temperatures with respect to its resonance frequency at 25.6 °C for each mode (Fig. 5c & 5d), we observe linear relation between $\Delta f/f$ and T among most of the measured temperatures, *i.e.*, from 10 to 105 ºC. In this range, we extract a TCf_1 of -336 ppm/K for the fundamental mode and TCf_2 of -316 ppm/K for the second mode. No clear trend of Q change is observed (Fig. 5g).

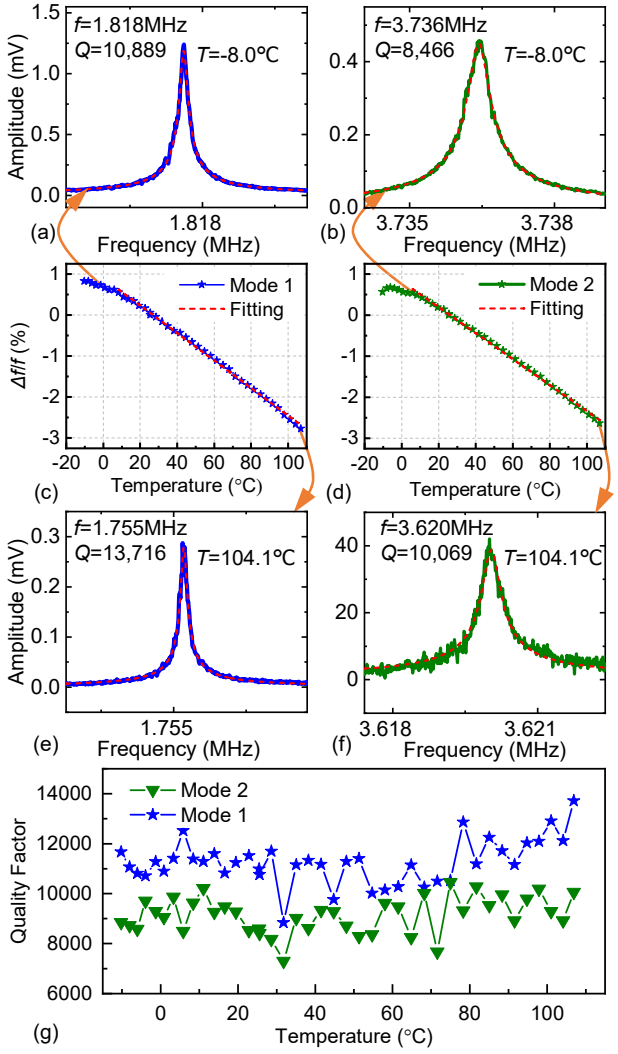

Figure 5: Measured out-of-plane mode resonances and TCf. Measured (a) first mode and (b) second mode resonances at -8.0 °C. (c) and (d) Fractional frequency shift with varying temperature. Measured (e) first mode and (f) second mode at 104.1 °C. (g) Dependence of measured Q on temperature, for the first two modes.

The multimode resonance frequency of a string is

$$f_n = \frac{n}{2L}\sqrt{\frac{\sigma}{\rho}} = \frac{n}{2}\sqrt{\frac{\sigma wt}{\rho wtL^2}} = \frac{n}{2}\sqrt{\frac{\sigma wt}{ML}}, \qquad (2)$$

where n is the mode number, M is the mass of the device and σ is the built-in stress in the string. According to the frequency ratio of the first two modes ($f_2/f_1 \approx 2$), the out-of-plane modes are precisely described by using this string model (with σ =700MPa). As temperature varies, the string's dimensions and built-in stress change due to thermal expansion, which shifts the resonance frequencies. The effect of thermal expansion can be described by deformation and stress modification of the string using the equations below

$$\begin{aligned} w &= w_0(1+\alpha T) \\ t &= t_0(1+\alpha T) \\ L &= L_0(1+\alpha_{Si}T) \\ \sigma &= \sigma_0 - (\alpha-\alpha_{Si})E_Y T \end{aligned}, \qquad (3)$$

where α and α_{Si} = 2.6 ppm/K are the thermal expansion coefficient for the GaN/AlN heterostructure and Si, respectively. Note that the effect of TCE_Y is not considered due to its negligible effect. By combining Eqs. (1)-(3), we have $\alpha \approx -2\sigma\cdot TCf/E_Y$. Thus, we obtain $\alpha \approx$ 4.6 ppm/K, which is comparable to α values of GaN (~2.0–3.8 ppm/K) and AlN (~4.2–5.3 ppm/K) from literature [9,10].

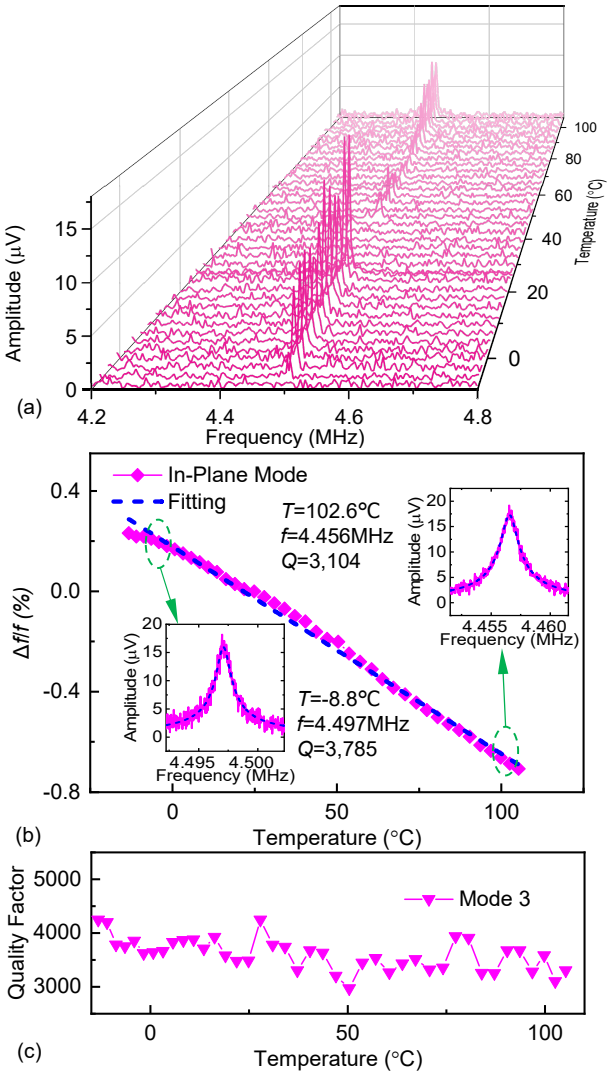

Figure 6: Measured in-plane flexural mode resonance and TCf. (a) Resonance spectra at different temperatures from -10 to 105°C. (b) Fractional frequency shift versus temperature. Insets show resonance spectra at selected temperatures. (c) Measured Q versus temperature.

To further investigate frequency response of the GaN/AlN doubly-clamped structure, we also measure the temperature dependence of the first in-plane (lateral) flexural mode (3rd mode overall, f_3). Figure 6a shows resonance spectra of the 3rd mode as the device temperature is regulated over T = -10 to 105 ºC. We observe much

smaller frequency shift as temperature varies (than in the earlier two modes). It is further confirmed by Fig. 6b, where f responds linearly to sweeping T in the measured T range with an averaged TCf_3 = -83 ppm/K, less than 1/3 of earlier measured values for out-of-plane modes (TCf_1 and TCf_2). Based on the cross-sectional shape (rectangular) and orientation of the doubly-clamped structure, the in-plane mode resonance frequency, f_3, depends more on E_Y of the material than on the built-in stress σ, compared to the two out-of-plane flexural modes (f_1 and f_2). Thus, the observation can be explained by the less efficient frequency modulation induced by Young's modulus change (governed by TCE_Y) than effect of built-in stress change (induced by thermal expansion). The Q of the in-plane mode is also stable upon varying temperature (Fig. 6c).

Furthermore, we characterize the effect of both 633nm red laser and 405nm blue laser on the fundamental mode resonance frequency of the GaN/AlN doubly-clamped resonator. When the laser spot is focused onto the device, a very small portion of the light can still be absorbed by the device (although for ideal GaN, $\lambda_{cutoff} = hc/E_g$ = 365nm, where h is Planck constant and c is the speed of light), which will result in parasitic heating from photothermal effect, thus inducing undesirable shift of resonance frequency. To quantify the parasitic frequency shift, we measure the resonance frequency at different red and blue laser power levels, as shown in Fig. 7. We find that the combined heating effect from both lasers could induce a resonance frequency downshift of ~6.9 kHz, which corresponds to a temperature increase (offset) of ~11.4 ºC. Although this may cause an offset in the f vs. T curves, the shapes and slopes of the curves remain unchanged; and according to Eq. (1), the TCf values obtained in Fig. 5 and Fig. 6 will remain the same even if the curves are offset.

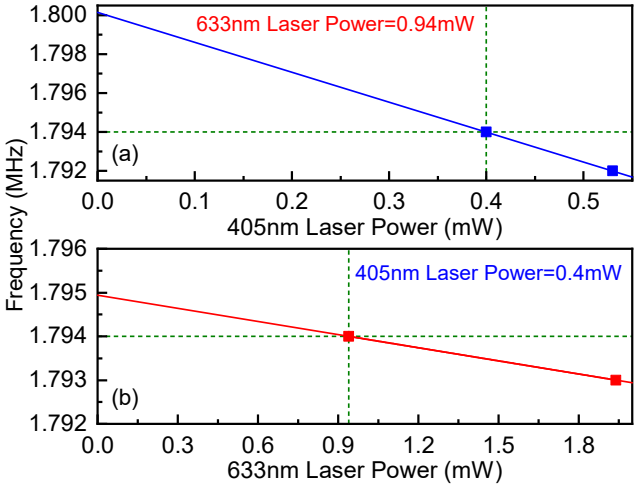

Figure 7: Calibration of the parasitic laser heating effect on frequency under varying (a) 405 nm and (b) 633 nm laser power on device. Scattered symbols: measured data. Solid lines: linear fitting. Dashed green lines indicate the conditions in the TCf measurements.

CONCLUSION

In summary, we have investigated the frequency response to temperature variation of two out-of-plane flexural modes and one in-plane flexural mode of a GaN/AlN heterostructure doubly-clamped resonator. We have extracted the TCf values for multimode resonance within the temperature range of -10 ºC to 105 ºC. We have obtained TCf_1 = -336 ppm/K for the fundamental out-of-plane mode and TCf_2 = -316 ppm/K for the second out-of-plane mode, which are much higher than that of the first in-plane mode (overall the third flexural mode), TCf_3 = -83 ppm/K. The dependence of TCf on resonance modes can play a key role in optimizing the device temperature stability. It can also be utilized for applications such as physical sensing based on thermal effects and frequency control in temperature varying environments.

ACKNOWLEDGEMENTS

We thank the financial support from the Defense Threat Reduction Agency (DTRA) Basic Scientific Research Program (Grant No. HDTRA1-19-1-0035 and Grant No. HDTRA1-15-1-0027).

REFERENCES

[1] O. Ambacher, "Growth and Applications of Group III-Nitrides", *J. Phys. D: Appl. Phys.*, vol. 31, pp. 2653-2710, 1998.

[2] S. P. DenBaars, D. Feezell, *et al.*, "Development of Gallium-Nitride-Based Light-Emitting Diodes (LEDs) and Laser Diodes for Energy-Efficient Lighting and Displays", *Acta Mater.*, vol. 61, pp. 945-951, 2013.

[3] A. Hassan, Y. Savaria, M. Sawan, "GaN Integration Technology, an Ideal Candidate for High-Temperature Applications: A Review", *IEEE Access*, vol. 6, pp. 78790-78802, 2018.

[4] M. Rais-Zadeh, V. J. Gokhale, *et al.*, "Gallium Nitride as an Electromechanical Material", *J. Microelectromech. Syst.*, vol. 23, pp. 1252-1271, 2014.

[5] A. Müller, D. Neculoiu, *et al.*, "6.3-GHz Film Bulk Acoustic Resonator Structures Based on a Gallium Nitride/Silicon Thin Membrane", *IEEE Electron Device Lett.*, vol. 30, pp. 799-809, 2009.

[6] M. Faucher, B. Grimbert, *et al.*, "Amplified Piezoelectric Transduction of Nanoscale Motion in Gallium Nitride Electromechanical Resonators", *Appl. Phys. Lett.,* vol. 94, art. no. 233506, 2009.

[7] C. Morelle, D. Théron, *et al.*, "Gallium Nitride MEMS Resonators: How Residual Stress Impacts Design and Performances", *Microsystem Technol.*, vol. 24, pp. 371-377, 2018.

[8] A. K. Samarao, F. Ayazi, "Temperature Compensation of Silicon Micromechanical Resonators via Degenerate Doping", in *Tech. Digest 2009 IEEE Int. Electron Device Meeting (IEDM)*, pp. 789-792, Baltimore, MD, Dec. 7-9, 2009.

[9] M. Leszczynski, T. Suski, *et al.*, "Thermal Expansion of Gallium Nitride", *J. Appl. Phys.*, vol. 78, pp. 4909-4911,1994.

[10] W. M. Yim, R. J. Paff, "Thermal Expansion of AlN, Sapphire, and Silicon", *J. Appl. Phys.*, vol. 45, pp. 1456-1457, 1974.

CONTACT

*Wen Sui: wen.sui@ufl.edu
*Bruce Alphenaar: bruce.alphenaar@louisville.edu
*Philip Feng: philip.feng@ufl.edu